Dynamics of two quantum entangled particles interacting with a potential barrier in an EPR experiment

Vittoria Petrillo*, Giorgia Alberti, Luca Celardo, Francesco Cerutti, Silvano Franchi, Vittorio Mariani

Istituto Nazionale di Fisica Nucleare, Dipartimento di Fisica,
Universit'a degli Studi di Milano,
20133 Milano, Italy

Abstract: The effect of a position measurement on one component of a two-particle wave packet in a regularized space-momentum entangled state is analyzed. The wave packet interacts in the physical space with a potential barrier. When a position or momentum measurement is performed on one particle, a consequent strong modification of the dynamics of the other particle occurs.
© Versita Warsaw and Springer-Verlag Berlin Heidelberg. All rights reserved.

1   Introduction

Entangled quantum states are not separable, even if their components are spatially far away from one another. This characteristic is usually referred to as non-locality, and it implies that measurements made on one part of the system influence the other instantaneously. The conflict between quantum mechanics and local realism that arises when entangled states are considered was the object of the famous work by Einstein, Podolsky and Rosen (EPR) [1]. In that paper, they introduced for the first time a gedanken experiment based on a couple of particles in a state entangled in position and momentum on which measurements of position and momentum are undertaken. They concluded about

* E-mail: Petrillo@mi.infn.it

the incompleteness of quantum mechanics, and envisaged also a possible violation of the Heisenberg uncertainty principle. This same problem was investigated by Bohm [2] in the case of a system of discrete variables with opposite conclusions, and led Bell [3] to the formulation of his inequalities relevant to the intrinsic quantum nature of a system. Bell himself said in a subsequent work [4] that for the continuous variables position and momentum it is not possible to derive analogous inequalities and that therefore the contradiction between quantum mechanics and local realism is, for these variables, not so easily made manifest as for the case of discrete states.

More recently, continuous-variables entangled states have been experimentally realized by means of parametric down-conversion [5, 6], with atomic ensembles interacting with light [7] or with squeezed beams of light [8]. Theoretical and experimental analysis has accurately studied the properties of these states [9–16], testing the violation of Bell inequality [17, 18], providing criteria for their separability [19–24] and showing the phenomenon of the ghost interference [25, 26].

In the present work, we consider a space-momentum entangled quantum state, describing couples of particles. We simulate a possible EPR experiment involving two particles in the presence of a potential barrier. In contrast to the case of EPR, we adopt a proper Gaussian wave function as the initial condition, which guaranties at each instant the correct normalization and the validity of the Heisenberg principle. In Section 2 we present the dynamics of this entangled system in the presence of semi-transparent and completely reflecting barriers. As the particles are initially anticorrelated in momentum, one particle of the pair travels towards the barrier and interacts with it, while the other propagates freely in the opposite direction. In Section 3 we consider the process of a position measurement made on one component of the system during its time evolution, with the aim of revealing the entanglement and the non-local correlations. When a measure of position is made, for instance, on the first particle, the dynamics of the second particle is considerably influenced, giving rise to several interesting phenomena which cannot be found in the motion of non-correlated pairs and that can be used for quantifying the entanglement of the system. The presence of the barrier introduces an element of asymmetry that opposes to the weakening of the entanglement and amplifies the changes in the dynamics of the particles that follow the measurement. In Section 4 measurements of momentum are shown. Discussions and conclusions are presented in Section 5.

2 Model equation and time evolution

We consider a two-particle system described by the Schroedinger equation :

$$i\frac{\partial \Psi(x_1, x_2, t)}{\partial t} = \hat{H}\psi(x_1, x_2, t)$$

$$\hat{H} = -\frac{1}{2}\frac{\partial^2}{\partial x_1^2} - \frac{1}{2}\frac{\partial^2}{\partial x_2^2} + V(x_1, x_2) \tag{1}$$

where $\psi(x_1, x_2, t)$ is the wave function of the system, x_1 and x_2 are the coordinates of the particles of the pair and the potential $V(x_1,x_2)$ is a barrier of height V_0 and depth a

defined by $V(x_1,x_2)=V_0$ if $0 < x_1 < a$ or if $0 < x_2 < a$ and 0 elsewhere.

As initial condition we consider an entangled wave function, superposition of EPR states, describing couples of particles that, in the same way as in EPR, are correlated in position and anticorrelated in momentum. We adopt normalized quantities. This state can be written in terms of the eigenfunctions of the operator $\mathbf{x}_1-\mathbf{x}_2$, namely $\delta(x_1-x_2-\xi)$, and of the operator total momentum $\mathbf{p}_1+\mathbf{p}_2$, namely the functions $e^{ip_{01}x_1+ip_{02}x_2}$, with eigenvalues $p_{01}+p_{02}=p_0$, as follows:

$$\psi(x_1, x_2, t = 0) = C \int d\xi \int dp_0\, e^{\frac{-\xi^2}{4\sigma_d^2}} e^{-\sigma_1^2 p_0^2}\, \delta(x_1 - x_2 - \xi)\, e^{ip_0 x_1 + ip_{02}(x_2 - x_1)}$$

$$= \frac{1}{\sqrt{2\pi\sigma_d\sigma_1}} e^{-\frac{(x_1-x_2)^2}{4\sigma_d^2} - \frac{x_1^2}{4\sigma_1^2} - ip_{02}(x_1 - x_2)} \tag{2}$$

The substantial difference between the state described by (2), and the δ function introduced by EPR [1] is that (2) is correctly normalized.

The wave function in the momentum representation turns out to be:

$$\phi(p_1, p_2) = \frac{\sqrt{2\sigma_d\sigma_1}}{\sqrt{\pi}} e^{-\sigma_d^2(p_2-p_{02})^2 - \sigma_1^2(p_1+p_2)^2} \tag{3}$$

In the present paper we have integrated numerically [27, 28] equation (1) with $\sigma_d = 0.5$ and $\sigma_1 = 1.5$, the initial position of both particles has been taken as $x_{01} = x_{02} = -10$, $p_0 = 10$, and a rectangular one-dimensional barrier of height V_0 has been positioned between $x_{1,2} = 0$ and $x_{1,2} = a$.

The choice made for σ_d and σ_1 guaranties that the initial function (2) is entangled with respect to the separability criteria proposed in the literature [20–25]. The entanglement marker defined by $\varepsilon = <\Delta(x_1 - x_2)^2><\Delta(p_1 + p_2)^2> / < |[x_1, p_1]| >$ is, in this case given by $\varepsilon = \sigma_d^2/\sigma_1^2 = 0,11 < 1/4$ while the covariance matrix takes the form

$$\underline{\underline{\Sigma}} = \begin{pmatrix} \underline{\underline{A}} & \underline{\underline{C}} \\ \underline{\underline{C^T}} & \underline{\underline{B}} \end{pmatrix} = \begin{pmatrix} \sigma_1^2 & 0 & \sigma_1^2 & 0 \\ 0 & \frac{1}{4}(\frac{1}{\sigma_1^2} + \frac{1}{\sigma_d^2}) & 0 & -\frac{1}{4\sigma_d^2} \\ \sigma_1^2 & 0 & \sigma_1^2 + \sigma_d^2 & 0 \\ 0 & -\frac{1}{4\sigma_d^2} & 0 & \frac{1}{4\sigma_d^2} \end{pmatrix} \tag{4}$$

so that the quantity S [21]

$$S = \det A \det B + (\frac{1}{4} - |\det C|)^2 - \mathrm{tr}(AJCJBJC^TJ) - \frac{1}{4}(\det A + \det B) \tag{5}$$

with $J = \begin{pmatrix} 0 & 1 \\ -1 & 0 \end{pmatrix}$, assumes at the initial instant, and during all the free propagation stage, before the impinging of the barrier, the negative value $S = -\frac{1}{4}\frac{\sigma_1^2}{\sigma_d^2}$. Two different cases have been studied starting from the same initial condition (2). First a semi-transparent barrier with $a = 1$ and $V_0 = 40$ has been considered, and then an opaque

completely reflecting barrier. The solution $\psi(x_1, x_2, t)$ of equation (1) is, of course, a complex function in the plane (x_1, x_2) and the motion in the physical space is analyzed by constructing the quantity:

$$P(x,t) = \int |\psi(x, \varsigma, t)|^2 d\varsigma \tag{6}$$

which represents the probability density that one particle be in the position x, independently of the position of the other particle.

An important factor of analysis is the Fourier transform of the wave packet, because it is connected with the composition in momentum of the packet.

The Fourier transform of the wave function with respect to one coordinate x_2 turns out to be:

$$\xi(p_2, x_1, t) = \frac{1}{\sqrt{2\pi}} \int dx_2 \Psi(x_1, x_2, t) e^{-ip_2 x_2} \tag{7}$$

and $|\xi(p_2, x_1, t)|^2$ represents the joint probability density that the first particle is in the position x_1, and the second particle has momentum p_2. Then, the integrated value:

$$\Pi(p_2, t) = \int |\xi(p_2, p_1, t)|^2 dp_1 \tag{8}$$

represents the probability density of finding particles with momentum p_2 in one of the two spatially separated components of the system.

As already stated, we start by analyzing the dynamics of a couple of entangled particle in the presence of a semi-transparent barrier of depth a=1 and height V_0=40. As the particles are initially anticorrelated in momentum, one of the particles travels towards the barrier, the other in the opposite direction.

Following the same conventional language used in the experiments with couples of photons we shall call signal the first wave packet and an idler the second. In Fig. 1 the time evolution of the modulus of the wave function $|\Psi(x_1, x_2, t)|$ in the plane x_1, x_2 is reported, showing the contour graphs at the time instants: Fig. 1(a) $t = 0$, Fig. 1(b) $t = 0.5$, Fig. 1(c) $t = 1$ Fig. 1(d) $t = 1.5$, Fig.1(e) $t = 2$ and Fig. 1(f) $t = 2.5$. The wave function propagates obliquely in the plane x_1, x_2 and the peak moves from the point $(-10, -10)$ at $t = 0$ towards the barrier as can be seen in Fig. 1(a) and 1(b). The first effect that can be noticed is the spread of the wave function.

As soon as the signal impinges on the barrier at $x_1 = 0$ it breaks into transmitted and reflected parts and looses the Gaussian shape. The reflection gives rise to interference fringes on the wave function on the left of the barrier (Fig. 1(c) and 1(d)).

Furthermore, a series of secondary peaks develop on the reflected part due to multiple reflections from the barrier. These secondary wave packets overlap the incident wave and interfere with it. It is also interesting to see the formation of the transmitted part, which first emerges symmetrically from the barrier and then distorts.

This distortion and the general asymmetry of the peaks and of the level curves can be observed in Fig. 1(e) and 1(f). This asymmetry is a consequence of the entanglement of the initial function because the term proportional to the factor $x_1 x_2$ in the exponent is responsible for the obliquity of the symmetry axes of the initial condition. This asymmetry is more accentuated for the reflected part, with respect to the transmitted one.
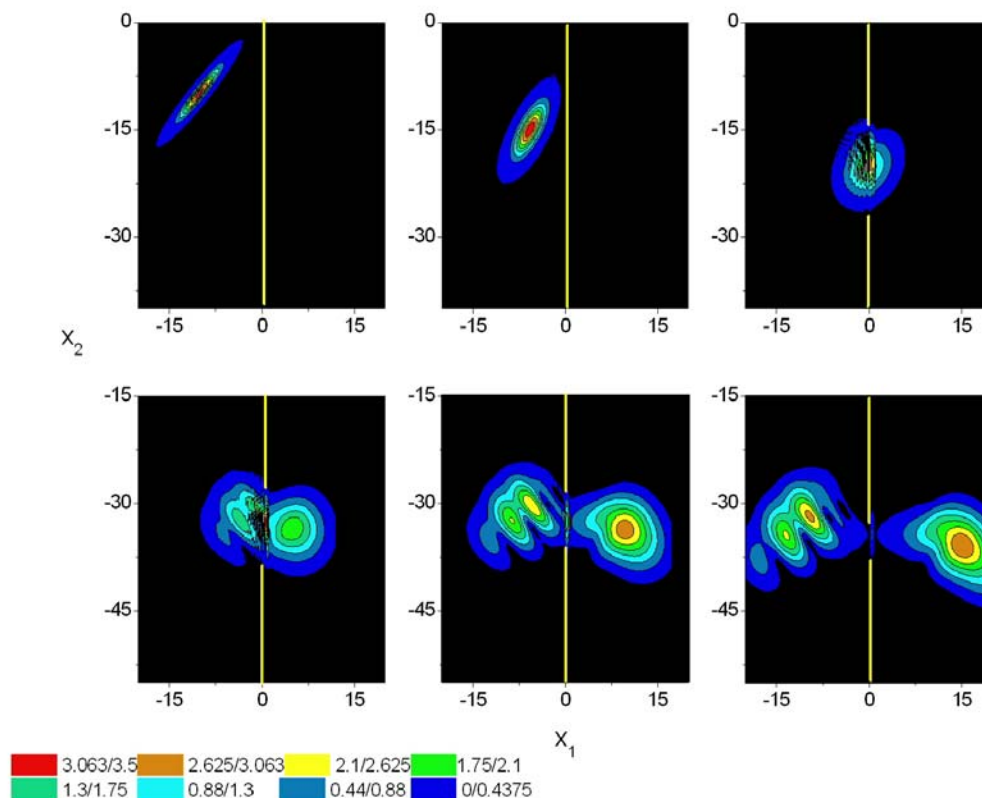
Fig. 1 Contour curves of the modulus of the wave function in the plane x_1, x_2 at (a) $t = 0$, (b) $t = 0.5$, (c) $t = 1$, (d) $t = 1.5$, (e) $t = 2$, (f) $t = 2.5$. The position of the barrier in $x_1 = 0$ is also drawn.

The multiple reflections yield the formation of islands. These islands have the major axis reversed with respect to that of the initial condition, and are aligned along their minor axis.

Another view of the dynamics of the system is given by the sequence of the integrated quantities P given by (6) for both particles, which is shown in Fig. 2 versus the position x in the laboratory for the same parameters and times as the preceding figures. In the integrated curves, many details present in the (x_1, x_2) plane are lost, particularly during and after the crossing of the barrier. In fact, the comparison, for instance, of Fig. 1(f) and Fig. 2(f), representing the same instant, shows to us how the structure of the joint probability $|\psi(x_1, x_2)|^2$ is more complicated than the probability density P in the physical space.

We can evaluate the spatial correlations of the wave function during the time evolution by means of the quantity

$$c(x_1, x_2) = |\psi(x_1, x_2)|^2 - p_x(x_1)p_x(x_2) \tag{9}$$
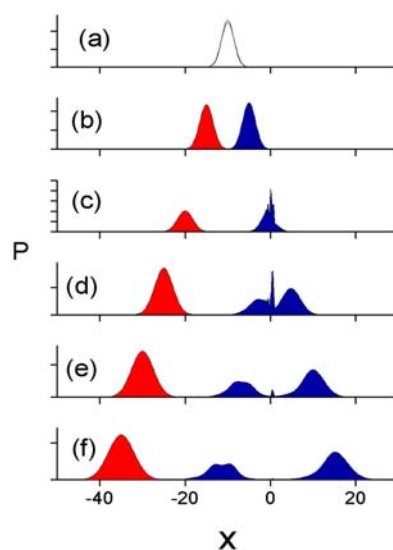
Fig. 2 Probability density P vs x of particle 1 (blue) and particle 2 (red) for the same parameter values as Figs 1, 2, 3 and (a) $t = 0$, (b) $t = 0.5$, (c) $t = 1$, (d) $t = 1.5$, (e) $t = 2$, (f) $t = 2.5$.

and by means of the global quantity:

$$C = \int |c(x_1, x_2)| dx_1 dx_2 \tag{10}$$

that can be calculated for the total wave function or separately for the transmitted and the reflected parts.

In Fig. 3 the quantity C is shown versus t for the total wave function in the presence of a barrier (a), for the reflected wave function (b), for the transmitted part (c) and, for comparison, for the free wave function (d), obtained in absence of a barrier. As can be seen, the presence of the barrier increases the correlations, especially when the reflected part is analyzed.

3 Position measurement

A position measurement on x_1, which localizes this particle in an interval δ around $\bar{x}_1$, projects the state of the system onto the wave function given by: $\bar{\psi}(x_1, x_2) = \psi(x_1, x_2)$ if $x_1 - \frac{\delta}{2} < x_1 < x_1 + \frac{\delta}{2}$ and 0 elsewhere.

The conditional probability density of having particle 2 in the position x_2 after this measurement turns out to be:

$$P^x(x_2, \bar{x}_1, \delta) = \int dx_1 \left| \bar{\psi} \right|^2 = \int_{\overline{x}_1 - \delta/2}^{\overline{x}_1 + \delta/2} dx_1 \left| \psi \right|^2 . \tag{11}$$

In Fig. 4 some position measurements on the transmitted part of the wave function of the signal are presented in the same case as Fig. 1, while Fig. 5 regards measurements
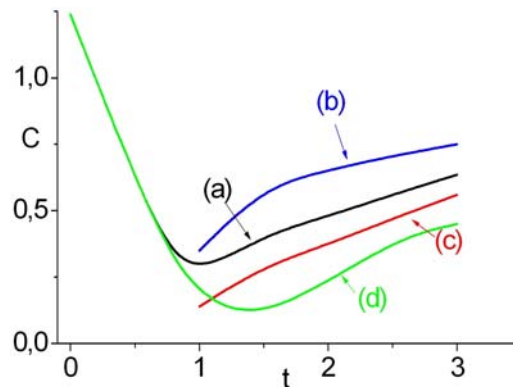
Fig. 3 Quantity C versus time t for the same parameter of Fig. 1; (a) for the total wave function, (b) for the reflected part, (c) for the transmitted part, and (d) for the free propagation case.

performed on the reflected part. In particular: Fig. 4 (a) represents the conditional probability density P^x for the signal on the right and for the idler on the left versus x, for a set of measurements made on x_1 for $2 < x_1 < 25$; in Fig. 4(b) x_1 ranges from 2 to 11; and in Fig. 4(c) $8 < x_1 < 9$. The measure on the transmitted part is felt by the idler in a limited way and the result is a shrinking of its probability density as in the usual EPR case.

A more intense effect is obtained if the measurement is made on the reflected part of the signal as shown in Fig. 5. In particular in Fig. 5(a) the measure is made on the whole reflected part for $-25 < x_1 < -1$. In Fig. 5(b) x_1 ranges between -9 and -1, while in Fig. 5(c) x_1 is from -5 to -4. In this case we do not have a shrinking of the conditional probability of the idler, but a strong deformation with the onset of large secondary peaks.

This effect is connected to the existence of the islands shown in Fig. 1(f) and to their disposition in the plane x_1, x_2. If we perform a cut along the x_2 axis we can provide evidence of the presence of these islands.

A further insight can be gained by observing the momentum distribution before and after the position measurements. In Fig. 6 (a) the integrated quantity Π for particle 2 versus p_2 is shown before the measurement.

In Fig. 6(b) this same quantity Π is represented after the thinner measurement made on the transmitted part with x_1 from 8 to 9 (as the case (c) of Fig. 4). In Fig. 6(c) the case of a thin measurement made on the reflected part (case (c) of Fig. 5, made on x_1 between -5 and -4) is presented. The measurement made on the transmitted part also has the effect of shrinking the momentum distribution, while the position measurement on the reflected part alters not only the shape of the probability density of particle 2, but in a drastic way all its future dynamics, because it produces the formation of two peaks with different values of momentum.

In fact, the spectrum Π of the conditional wave function just after the measurement
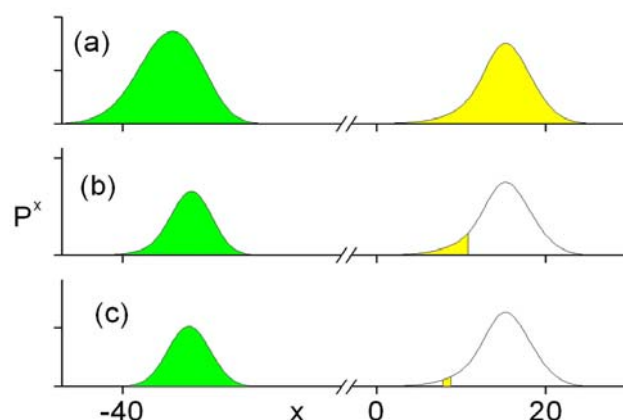
Fig. 4 Conditional probability density P^x vs. x for particle 1 (green) and particle 2 (yellow) after position measurements on x_1: (a) $2 < x_1 < 25$, (b) $2 < x_1 < 11$, (c) $8 < x_1 < 9$.
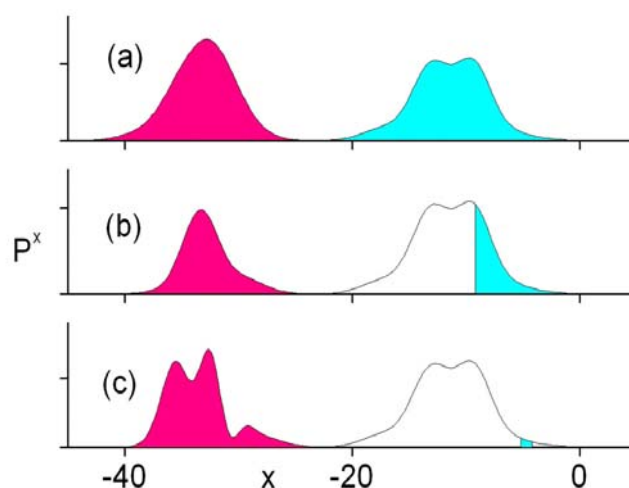
Fig. 5 Conditional probability density P^x vs. x for particle 1 (pink) and particle 2 (cyan) after position measurements on x_1: (a) $-25 < x_1 < -1$, (b) $-9 < x_1 < -1$, (c) $-5 < x_1 < -4$.

presents a structure with two peaks, generating two separate wave packets with two different average values of momentum. The peak at the right represents an ensemble of particles with smaller velocity that will travel more slowly with respect to the others.

In fact if we evolve in time the wave function after the position measurement represented in Fig. 5(c) and 6(c) looking at what happens to the idler, we can see clearly the spatial fragmentation in two principal packets propagating with different momentum. A snapshot of the probability density P^x of the idler versus x at $t = 4$ after the measurement is presented in Fig. 7. After the measurement, the correlations between the two particles
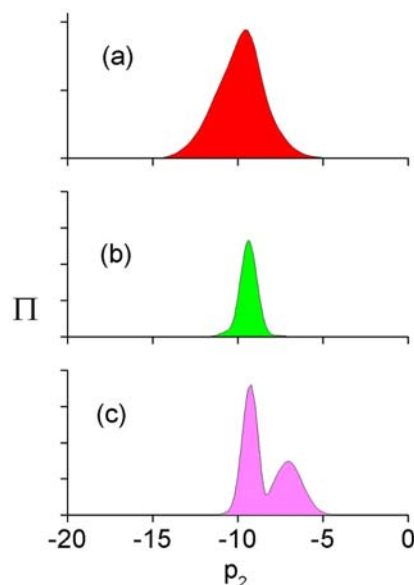
Fig. 6 Momentum probability density vs. p_2 at $t = 2.5$, (a) without measurement, (b) $8 < x_1 < 9$, (c) $-5 < x_1 < -4$.
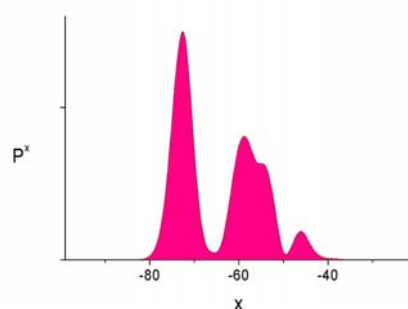
Fig. 7 P^x vs. x for the same case of Fig. 5 (c) at a time $t = 4$ after the position measurement.

become very weak and the time evolution is therefore substantially governed by a one particle Schroedinger equation.

We now analyze the case of an opaque barrier. In Fig. 8 the contour graph of the modulus of the wave function is presented in the x_1, x_2 plane for $a = 1$, $V_0 = 5000$, $\sigma_1 = 1.5$, $\sigma_d = 0.5$ at the instant of the interaction with the barrier at $t = 1$. Also in this case we can recognize the formation of islands inclined in the x_1, x_2 plane. The position measurement is made between the two white lines in the picture corresponding to $x_1 = -7$ and $x_1 = -6$. Also in this case there is the possibility of connecting the entanglement of the initial wave function with the behavior of the second particle after the position measurement on the first.

In fact if we perform the Fourier transform of the conditional wave function we obtain
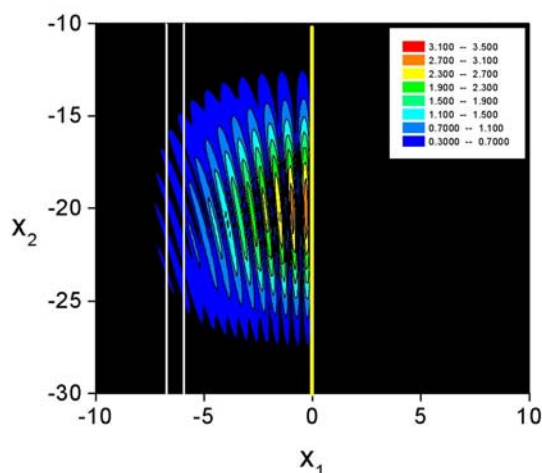
Fig. 8 Contour curves of the modulus of the wave function in the plane x_1, x_2 at $t = 1$ for $V_0 = 5000$. The position of the barrier at $x_1 = 0$ and the interval of the position measurement between $x_1 = -6$ and $x_1 = -7$ are also drawn.
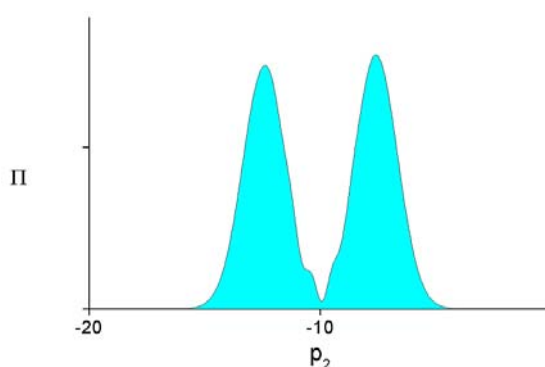
Fig. 9 Π vs p_2 after the position measure between $x_1 = -6$ and $x_1 = -7$ for the same case as Fig. 8.

for the integrated quantity Π vs p_2 the result shown in Fig. 9, with the characteristic two peaked shape. The time evolution of the system after the position measurement is presented in Fig. 10, where the probability density P^x of particle 2 is presented as a function of x at the time instant immediately before the measurement (a), and after $\Delta t = 1$ from the measurement (b). Also in this case the idler separates into two packets that in time move away from eachother.

4   Momentum measurement

The momentum measurement implies a cut of the Fourier transform of the wave packet. In Fig. 11 the spatial probability density conditioned by a momentum measurement P^P is shown as a function of x for three different cases. In Fig. 11(a) the measure is made
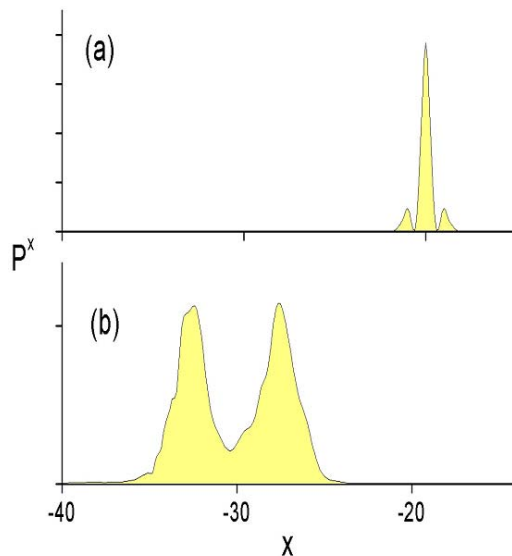
Fig. 10 P^x vs. x, for the same case as Fig. 8 and 9, (a) just after the measurement and (b) after a time $\Delta t = 1$.

on p_1 between -15 and 0, in Fig. 11 (b) p_1 ranges between -7 and -3 and in Fig. 11(c) p_1 is between -9 and -8.5.

In Fig. 12 an analogous case is presented, but with measurements made on the positive momentum component. In fact in Fig. 12 (a) p_1 ranges from 0 to 15, in Fig. 12 (b) $3 < p_1 < 7$ and in Fig. 12 (c) p_1 is between 5 and 5.5.

In analogy with the position measurement we can observe that the measurement made on the transmitted part of the signal (in this case on particles with positive momentum) produces a less important distortion on the idler, while the cut made on the reflected part is felt strongly by particle 2.

5   Conclusions

We have simulated the time evolution and the process of position and momentum measurements on an entangled two particles system interacting with a potential barrier. The initial wave packet is constituted by couples of particles correlated in position and anticorrelated in momentum in a similar way as in EPR. In the physical space we see one particle (called the idler) going freely towards the left and the other particle (the signal), that propagates towards right, impinging on the barrier. If the insertion of a semitransparent barrier on the trajectory of one particle is analyzed, the wave packet that encounters the barrier separates into transmitted and reflected parts. On the contrary, in the case of a completely reflecting barrier all the wave function is reflected. We can imagine performing position measurements on the signal, either on the right of the potential barrier, observing the particles transmitted, or on the left of the barrier intercepting the reflected
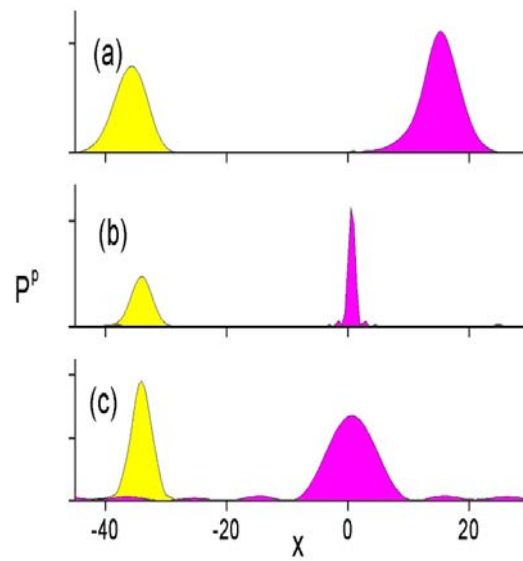
Fig. 11 Spatial probability density conditioned by a momentum measurement P^P vs. x for a momentum measurement made on (a) p_1 between -15 and 0, (b) p_1 ranges between -7 and -3 and (c) p_1 is between -9 and -8.5.
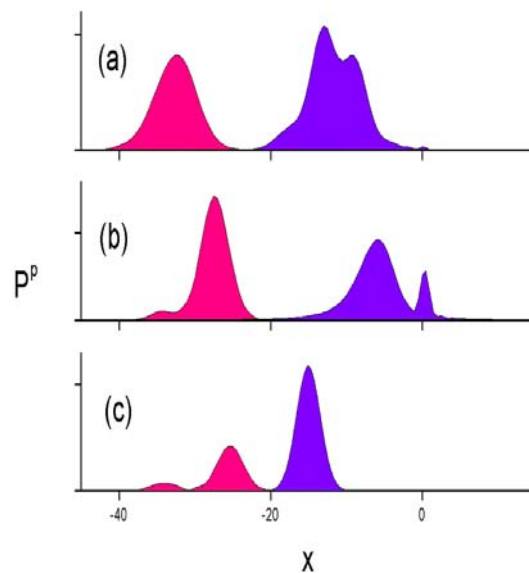
Fig. 12 Spatial probability density conditioned by a momentum measurement P^P vs. x for a momentum measurement made on (a) p_1 ranges from 0 to 15, (b) $3 < p_1 < 7$ and (c) p_1 is between 5 and 5.5.

particles.

The idler, which is supposed to travel freely towards the left far from the first particle

and far from the barrier, strongly feels the position measurement on the first particle, as predicted by EPR. Its reaction, however, is different if the transmitted or the reflected wave packet is measured. In the first case a reshaping of the wave packet with a shrinking of its width is achieved in agreement with the EPR predictions, while, if the reflected wave packet is measured, a drastic upset of all the dynamics of the second particle occurs. In fact, in this last case, we observe the formation of two separate wave packets with different average momentum values that in time move away from one another. The same phenomenon is seen if the wave packet collides with an opaque barrier. The observation of more than one wave packet for the idler when a position measurement is made on particle 1 is clearly a consequence of the non-local correlations present in the initial wave function and can be used to evaluate its degree of entanglement.

Acknowledgment

References

[1] A. Einstein, B. Podolsky and N. Rosen: "Can Quantum-Mechanical Description of Reality Be Considered Complete?", *Phys. Rev. Series II*, Vol. 47, (1935), pp. 777-780

[2] D. Bohm: *Quantum Theory*, Prentice Hall, Englewood Cliffs, 1951.

[3] J.S. Bell: "On the Einstein Podolsky Rosen Paradox", *Physics* , Vol. 1, (1964), p. 195.

[4] J.S. Bell: *Speakable and unspeakable in quantum mechanics*, Cambridge University Press, Cambridge, U.K., 1987.

[5] H.J. Kimble and D.F Walls: "Special issues on squeezed states of light", *J. Opt. Soc. Am. B*, Vol. 4, (1987), pp. 1450–1741

[6] A. Lamas-Linares, J.C. Howell and R.D. Bouwmeester: "Stimulated emission of polarization-entangled photons", *Nature*, Vol. 412, (2001), pp. 887–890.

[7] B. Julsgaard , A. Kozhekin and E.S. Polzik: "Experimental long-lived entanglement of two macroscopic objects", *Nature*, Vol. 413, (2001), pp. 400–403.

[8] Ch. Silberhorn, P.K. Lam, O.Weiss, F. Koenig, N. Korolkova and G. Leuchs: "Generation of Continuous Variable Einstein-Podolsky-Rosen Entanglement via the Kerr Nonlinearity in an Optical Fiber", *Phys. Rev. Lett.*, Vol. 86, (2001), pp. 4267–4270.

[9] M.D. Reid and P.D. Drummond: "Quantum Correlations of Phase in Nondegenerate Parametric Oscillation", *Phys. Rev. Lett.*, Vol. 60, (1988), pp. 2731–2735.

[10] M.D. Reid: "Demonstration of the Einstein-Podolsky-Rosen paradox using nondegenerate parametric amplification", *Phys. Rev. A*, Vol. 40, (1089), pp. 913–923.

[11] K. Banaszek and K. Wódkiewicz: "Nonlocality of the Einstein-Podolsky-Rosen state in the Wigner representation", *Phys. Rev. A*, Vol. 58, (1998), pp. 4345–4347.

[12] A.S. Parkins and H.J. Kimble: "Position-momentum Einstein-Podolsky-Rosen state of distantly separated trapped atoms", *Phys. Rev. A*, Vol. 61 , (2000), art. 052104.

[13] S. Lloyd, J.H. Shapiro and F.N.C. Wong:"Quantum magic bullets by means of entanglement", *J. Opt. Soc. Am. B*, Vol. 19, (2002), pp. 312–318.

[14] Z.Y. Ou, F. Pereira, H.J. Kimble and K.C. Peng: " Realization of the Einstein-Podolsky-Rosen paradox for continuous variables", *Phys. Rev. Lett.*, Vol. 68, (1992), pp. 3663–3666.

[15] Z.Y. Ou, S.F. Pereira and H.J. Kimble: "Realization of the Einstein-Podolsky-Rosen paradox for continuous variables in nondegenerate parametric amplification", *Appl. Phys. B*, Vol. 55, (1992), pp. 265–278.

[16] J.F. Clauser and A. Shimony: "Bell's theorem. Experimental tests and implications", *Rep. Prog. Phys.*, Vol. 41, (1978), pp. 1881–1927.

[17] A. Aspect, P. Grangier and G. Roger: "Experimental Tests of Realistic Local Theories via Bell's Theorem", *Phys. Rev. Lett.*, Vol. 47, (1981), pp. 460–463.

[18] M. D. Reid: "Violations of Bell inequalities for measurements with macroscopic uncertainties: What it means to violate macroscopic local realism", *Phys. Rev. A*, Vol. 62, (2000), art. 022110.

[19] A. Peres: "Separability Criterion for Density Matrices", *Phys. Rev. Lett.*, Vol. 77, (1996), pp. 1413–1415.

[20] P. Horodecki: "Separability criterion and inseparable mixed states with positive partial transposition", *Phys. Lett. A*, Vol. 232, (1997), pp. 333–339.

[21] R. Simon: "Peres-Horodecki Separability Criterion for Continuous Variable Systems", *Phys. Rev. Lett.*, Vol. 84, (2000), pp. 2726–2729.

[22] Lu-Ming Duan, G. Giedke, J.I. Cirac and P. Zoller: "Inseparability Criterion for Continuous Variable Systems", *Phys. Rev. Lett.*, Vol. 84, (2000), pp. 2722–2725.

[23] S. Mancini, V. Giovannetti, D. Vitali and P. Tombesi : "Entangling Macroscopic Oscillators Exploiting Radiation Pressure", *Phys. Rev. Lett.* , Vol. 88 , (2002), art. 120401.

[24] M. D'Angelo, Yo-Ho Kim, S.P. Kulik and Y. Shih: "Identifying Entanglement Using Quantum Ghost Interference and Imaging", *Phys. Rev. Lett.*, Vol. 92, (2004), art. 233601.

[25] D.V. Strekalov, A.V. Sergienko, D.N. Klyshko and Y.H. Shih: "Observation of Two-Photon "Ghost" Interference and Diffraction", *Phys. Rev. Lett.*, Vol. 74, (1995), pp. 3600–3603.

[26] T.B. Pittman, Y.H. Shih , D.V. Strekalov and A.V. Sergienko: "Optical imaging by means of two-photon quantum entanglement", *Phys. Rev. A*, Vol. 52, (1995), pp. R3429–R3432.

[27] J.J.V. Maestri , R.H. Ladau and M.J. Paez: "Two-Particle Schroedinger Equation Animations of Wavepacket-Wavepacket Scattering", *Am. J. Phys.*, Vol. 68, (2000), pp. 1113–1118.

[28] T. Iitaka: "Solving the time-dependent Schrödinger equation numerically", *Phys. Rev. E*, Vol. 49, (1994), pp. 4684–4690.